



COBEM
2021 Florianópolis - Brasil



26th ABCM International Congress of Mechanical Engineering
November 22-26, 2021. Florianópolis, SC, Brazil

COB-2021-0265

NUMERICAL ANALYSIS OF A SAVONIUS TURBINE INSERTED IN OSCILLATING WATER COLUMN WAVE ENERGY CONVERTER

Andrei Luís Garcia Santos

Federal University of Rio Grande – FURG, Av. Itália, km 8, s/n, CEP 96203-900, Rio Grande, RS, Brazil
andrei_eng_mec@hotmail.com

Filipe Branco Teixeira

Federal University of Rio Grande do Sul – UFRGS, St. Sarmiento Leite, 425, CEP 90150-170, Porto Alegre, RS, Brazil
fbrancoteixeira@gmail.com

Liércio André Isoldi

Federal University of Rio Grande – FURG, Av. Itália, km 8, s/n, CEP 96203-900, Rio Grande, RS, Brazil
liercioisoldi@furg.br

Jeferson Avila Souza

Federal University of Rio Grande – FURG, Av. Itália, km 8, s/n, CEP 96203-900, Rio Grande, RS, Brazil
jasouza@furg.br

Mateus das Neves Gomes

Federal Institute of Paraná – IFPR, St. Antônio Carlos Rodrigues, 453, CEP 83215-750, Paranaguá, PR, Brazil
mateus.gomes@ifpr.edu.br

Luiz Alberto Oliveira Rocha

University of Vale do Rio dos Sinos – UNISINOS, Av. Unisinos, 950, CEP 93022-750, São Leopoldo, RS, Brazil
luizor@unisinos.br

Elizaldo Domingues dos Santos

Federal University of Rio Grande – FURG, Av. Itália, km 8, s/n, CEP 96203-900, Rio Grande, RS, Brazil
elizaldosantos@furg.br

Abstract. This work presents a numerical analysis of a turbulent flow over a Savonius turbine in a domain that mimics an Oscillating Water Column (OWC) device. The model includes a dynamic mesh simulation on which the turbine angular velocity is prescribed. The geometry is investigated using Constructal Design, being considered a constant area (A_1) for the chamber and two degrees of freedom. Here, the effect of the turbine duct positioning on the equipment, represented by the ratio between the distance from the position of the water-free surface to the turbine duct center and the height of the OWC device (H_2/H_1), on the resulting power coefficient is evaluated. For all cases, the height/length ratio of the chamber is constant ($H_1/L_1 = 0.55$). The study is carried out considering a two-dimensional domain, where the OWC device contains the turbine duct on the side of its chamber. The airflow in the domain is caused by the imposition of a constant velocity $V_{cte} = 1.4$ m/s at the lower surface of the OWC chamber. Moreover, a turbine rotor constant velocity $\omega' = 15.5$ rad/s is imposed in the Savonius turbine. The computational mesh was generated with the GMSH software. To solve the turbulent flow, the time averaged equations of mass conservation and balance of momentum are solved numerically with the finite volume method (FVM), more precisely with the Ansys Fluent 18.1 commercial software. For closure of turbulence, it is considered the $k-\omega$ SST Reynolds-Averaged Navier Stokes (RANS) method. A comparison between present method and results of literature for a case with free Savonius turbine was performed to verify the solution. The studied cases of OWC with turbine were also compared with similar domains and without inserted turbine with the aim to investigate the influence of the model simplification in the performance and design of the device. For the present conditions, the highest power take off (PTO) on the device and available power were obtained for the highest magnitude of the ratio H_2/H_1 ($H_2/H_1 = 0.81$). Moreover, the effect of the ratio H_2/H_1 over the PTO and available power for the conditions with and without turbine were similar, indicating that the improvement of the model (considering the turbine) was important only for prediction of PTO and not for the recommendation about the best configuration of the device.

Keywords: OWC, Numerical Simulation, Savonius Turbine, Turbulent Flows, Constructal Design.

1. INTRODUCTION

Electric energy from renewable sources is a fundamental issue to be addressed nowadays. Its importance is not only concerned with the environmental preservation, but also with economic issues of energy generation. According to Aneel (2021), over the last five years, in Brazil, the consumed power electricity from fossil sources (non-renewable) and from water falls (that can lead to great costs and environmental impacts) were 21,823.55 MW, while renewable power sources (wind, biomass and solar energies), together, add up to 16,386.35 MW.

The ocean energy conversion into electricity has been the target of an increasing number of scientific works, focusing on boosting the energy matrix, in turn, reducing demand for non-renewable and high-cost fuels. According to Jenniches (2018) the transition from current sources to renewable energy is one of the main trends, as well as, the diversification in ways to convert renewable energy into available energy for human consumption.

In this sense, the search for scientific and technological advances on the comprehension of the physical phenomenology of Wave Energy Converters (WEC) as the Oscillating Water Column (OWC) device has been intensified. This device represents a relatively simple way to provide the mechanical energy conversion from waves movement into electricity through an inserted turbine in the equipment. According to Twidell and Weir (2015), the OWC converter can be defined as a device containing a hydropneumatic chamber with at least two openings, one in communication with the atmosphere and another in communication with the sea. When the water column inside the hydropneumatic chamber oscillates due to the wave movement it causes compression and decompression of air inside the chamber above the water-free surface. The mass flow rate of air is forced to exit by a duct or entering from atmosphere to the chamber in compression and decompression stages, passing through the turbine that converts mechanical energy into electricity.

In order to reduce the computational effort, a two-dimensional analysis has been performed to determine the geometric shapes that improve the OWC equipment performance. For instance, Pinto Jr. *et al.* (2019) evaluated the behavior of static pressure in an OWC by varying the width of the equipment turbine duct. The model considered only the region of the chamber and the equipment duct subjected to a turbulent airflow. Moreover, the interaction between the wave flow in the channel is not considered and the influence of wave flow over the chamber is simulated by imposition of a velocity in the lower surface of the chamber.

Other contributions were being recommended considering the OWC device installed inside a wave channel. For instance, Letzow *et al.* (2020) studied, by means of Constructal Design and exhaustive search method the performance of an onshore device, i.e., a device installed at the end of the numerical wave channel (which simulates the oceanic coast). In this work, the performance indicator was the available power since there is no turbine or restriction imposed at the duct. In spite of some simplifications adopted in this work, geometry proved to be an important issue for design of OWC devices.

Constructal Design is a method based in a physical principle named Constructal Law. According to Bejan (2018), the principle states that for a flow system with finite dimensions to persist in time, its configuration must freely evolve in order to easily the access of the currents that flow through the system. It is important to emphasize that Constructal Design is a physical principle that addresses geometric shapes to be studied (defining the search space of investigation). However, for geometric optimization, it is necessary to associate an optimization technique. In the work of Letzow *et al.* (2020) the exhaustive search method was used to optimize the ratio between the height and the length of the hydropneumatic chamber of the equipment for two different lengths of frontal device wall, i.e., obtaining the configuration that maximizes the available power of the OWC.

The Savonius turbine was widely used for generation of wind energy (Savonius, 1930). In this way, it is also worth mentioning two studies about the computational modeling of Savonius impulse turbines with dynamic mesh. In the work of Akwa (2010), the experimental research carried out by Blackwell *et al.* (1977) was reproduced in such way to validate the used computational modeling. In this work, the Savonius turbine has its aerodynamics coefficients analyzed acting in a wind tunnel. Afterwards, Dos Santos *et al.* (2019) verified another numerical method, based in the implementation of Finite Volume Method (FVM) in FLUENT using the previous numerical results of Akwa (2010). In a second moment, the same turbine studied in the verification case (free turbine in a wind tunnel) was used in a domain similar to that observed in an OWC device, i.e., an enclosed domain. It was investigated the influence of consider an enclosed domain for prediction of drag, lift, momentum and power coefficients.

In present work, main purpose is to analyze the influence of some geometric configuration of the OWC device over the device performance considering a Savonius turbine inserted in the OWC duct. At the authors knowledge, this kind of investigation was not previously performed in another works reported by literature. More precisely, it is considered a horizontal turbine duct placed in lateral side of the chamber. The turbine duct position is varied and its effect over the RMS (Root Mean Square) power coefficient is investigated. Details about RMS calculation can be seen in Marjani *et al.* (2006) and Letzow *et al.* (2020). Another objective is to analyze the efficiency obtained by each of the geometric variations of the analyzed equipment in relation to the available power i.e., without the presence of the Savonius turbine in the OWC device duct.

The computational meshes are generated with the GMSH software and the solution of governing equations is performed with the Ansys FLUENT 18.1 commercial code. Constructal Design is used to define the search space of studied cases and the exhaustive search is employed for geometric optimization. Here, the study is limited to the OWC

duct position influence over the RMS power coefficient for the case with inserted turbine and over the RMS available power for the case without inserted turbine. It is important to note that, in present work, only one degree of freedom (DOF) is evaluated as a first assessment to perform a geometric investigation of the simplified device with the inserted Savonius turbine in the domain that mimics the OWC device.

2. MATHEMATICAL AND NUMERICAL MODELING

In this paper, flow is simulated as turbulent and incompressible in a two-dimensional domain and transient regime, with constant thermophysical properties and $k-\omega$ SST turbulence model. The equipment duct is arranged in the horizontal direction, next to the hydropneumatic chamber, similarly to the configuration studied in Letzow *et al.* (2020). The geometry can be checked in Figure 1.

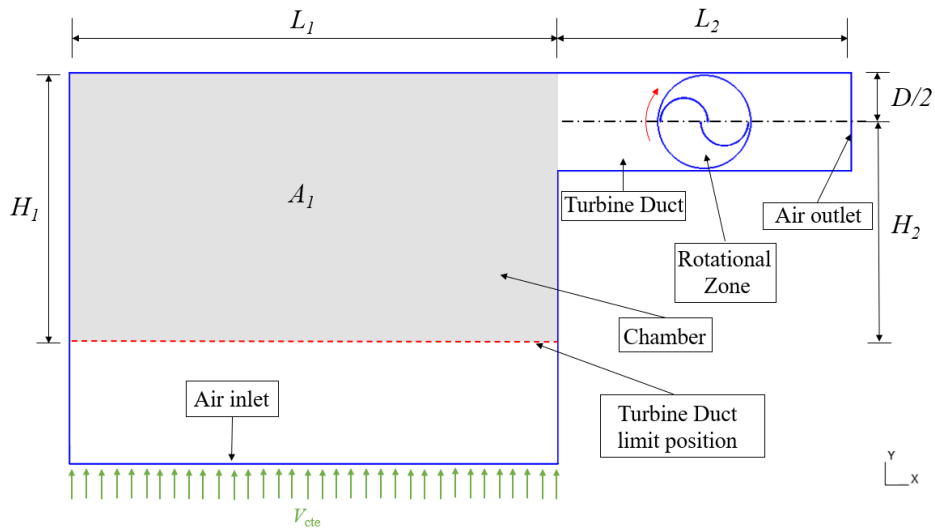


Figure 1. Case study: OWC with horizontal turbine duct.

The geometry is analyzed in order to obtain, as performance indicator, the RMS power coefficient by varying the device duct position through several simulations, where, $L_1 = 10$ m, $L_2 = 6$ m, $D = 2$ m, $H_1 = 5.5$ m and H_2 is variable in a ratio H_2/H_1 . The area A_1 is constant and given by $A_1 = H_1 \cdot L_1$.

The boundary conditions of the problem are no-slip and impermeability at the chamber and the duct walls, $V_{cte} = 1.4$ m/s at the OWC inlet line and atmospheric pressure at the duct outlet line. The inlet velocity magnitude is the same adopted in the work of Dos Santos *et al.* (2019). This allow to prescribe a velocity at the duct similar in magnitude with that used in the verification and mesh independent test section. A rotational moving mesh domain mimics a Savonius turbine rotor. The turbine is placed in the OWC duct center, $L_2/2$. Moreover, it is considered a diameter of turbine with $d = 1.8$ m and the blades have a thickness of $e = 0.0072$ m. The blades overlay is $S = 0.144$ m and their chords size is $C = 0.972$ m, as illustrated in Figure 2.

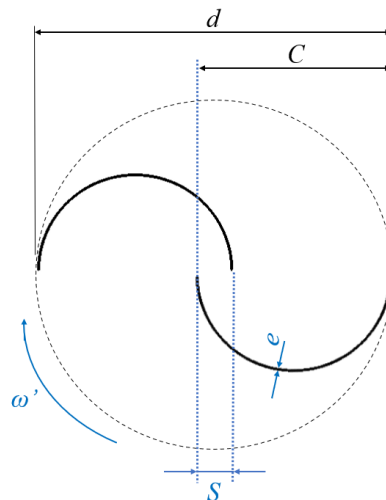


Figure 2. Savonius turbine rotor measurement parameters.

For all the simulations, the constant rotor angular velocity is $\omega' = 15.5$ rad/s and the turbine rotor tip speed ratio is $\lambda = 2$. In this problem, the time-averaged equations of mass conservation and balance of momentum in the x and y coordinates are addressed and solved applying the Finite Volume Method (FMV) discretization seen in Versteeg and Malalasekera (2007), Patankar (1980) and Maliska (2004). In this sense, these equations are respectively:

$$\frac{\partial u_i}{\partial x_i} = 0 \quad (1)$$

$$\rho \frac{\partial u_i}{\partial t} + \rho u_j \frac{\partial u_i}{\partial x_j} = - \frac{\partial p_i}{\partial x_i} + \frac{\partial}{\partial x_j} \left(\mu \frac{\partial u_i}{\partial x_j} \right) + \rho g_i \quad (2)$$

where x_i and x_j [m] are the spatial coordinates, u_i and u_j [m/s] are the velocity components and g_i [m/s²] is the gravity. The constant thermophysical air density and dynamic viscosity properties are respectively: $\rho = 1.18415$ kg/m³ and $\mu = 1.7894 \times 10^{-5}$ kg/m·s.

According to Menter *et. al.* (2003) and Wilcox (2004), for k - ω SST turbulence model, a turbulent viscosity is given by:

$$\mu_t = \frac{\bar{\rho} \alpha_1 k}{\max(\alpha_1 \omega, SF_2)} \quad (3)$$

The turbulent kinetic energy generation is expressed by:

$$\frac{\partial k}{\partial t} + \frac{\partial (u_i k)}{\partial x_i} = \tilde{P}_k - \frac{k^{3/2}}{L_T} + \frac{\partial}{\partial x_i} \left[(\mu + \sigma_k \mu_t) \frac{\partial k}{\partial x_i} \right] \quad (4)$$

where u_i [m/s] is the horizontal direction velocity, \tilde{P}_k is a term that prevent the turbulence generation in stagnation regions and L_T is the turbulent length scale of a Cartesian grid.

The specific dissipation rate is calculated by:

$$\frac{\partial \omega}{\partial t} + \frac{\partial (u_i \omega)}{\partial x_i} = \left(\frac{\alpha}{\mu_t} \right) \tilde{P}_k - \beta \omega^2 + \frac{\partial}{\partial x_i} \left[(\mu + \sigma_\omega \mu_t) \frac{\partial \omega}{\partial x_i} \right] + 2(1 - F_1) \frac{\sigma_{\omega 2}}{\omega} \frac{\partial k}{\partial x_i} \frac{\partial \omega}{\partial x_i} \quad (5)$$

The F_1 and F_2 blending functions seen in Eq. (4) and (6) are calculated by:

$$F_1 = \tanh \left\{ \left\{ \min \left[\max \left(\frac{\sqrt{k}}{\beta^* \omega y}, \frac{500v}{y^2 \omega} \right), \frac{4\rho \sigma_{\omega 2} k}{CD_{k\omega} y^2} \right] \right\}^4 \right\} \quad (6)$$

where $CD_{k\omega}$ is given by:

$$CD_{k\omega} = \max \left(2\rho \sigma_{\omega 2} \frac{1}{\omega} \frac{\partial k}{\partial x_i} \frac{\partial \omega}{\partial x_i}, 10^{-10} \right) \quad (7)$$

and

$$F_2 = \tanh \left[\left[\max \left(\frac{2\sqrt{k}}{\beta^* \omega y}, \frac{500v}{y^2 \omega} \right) \right]^2 \right] \quad (8)$$

In Eq. (3) – (8), k is the turbulent kinetic energy [m²/s²], v [m/s] is the velocity in y direction, ω is the specific dissipation rate, μ_t is the turbulent viscosity, $\alpha_1 = 5/9$, $\beta = 0.09$, $\beta_1 = 3/40$, $\beta_2 = 0.0828$, $\sigma_2 = 0.44$, $\sigma_k = 0.85$, $\sigma_\omega = 0.5$ and $\sigma_{\omega 2} = 0.856$.

2.1 Power coefficient

The available power in the problem used to calculate the power coefficient in the Savonius turbine is calculated by (Cresesb, 2008):

$$P_{available} = \frac{1}{2} \cdot \rho \cdot A_{duct} \cdot V_{cte}^3 \quad (9)$$

where A_{duct} [m²] is the OWC device duct cross section area without a turbine presence and V_{cte} is the constant velocity at the inlet of the domain.

To perform the power transmitted to the turbine, $P_{turbine}$, the same author presents the following equation:

$$P_{turbine} = \frac{1}{2} \cdot \rho \cdot A_{duct} \cdot V_{cte}^3 \cdot \left[\frac{1}{2} \cdot \left(1 + \frac{V_{at}}{V_{cte}} \right) \cdot \left(1 - \left(\frac{V_{at}}{V_{cte}} \right)^2 \right) \right] \quad (10)$$

where V_{at} is the air velocity after flowing through the Savonius turbine blades.

The power coefficient, C_p , that represents the ratio between the turbine's shaft transmitted power and the airflow available power without the turbine presence is:

$$C_p = \left[\frac{1}{2} \cdot \left(1 + \frac{V_{at}}{V_{cte}} \right) \cdot \left(1 - \left(\frac{V_{at}}{V_{cte}} \right)^2 \right) \right] = \frac{P_{turbine}}{P_{available}} \quad (11)$$

To perform the calculations, the $C_{p_{RMS}}$ (Root Mean Square) was used, which according to Letzow *et al.* (2020), Gomes (2014) and Marjani *et al.* (2006) is obtained by:

$$C_{p_{RMS}} = \sqrt{\frac{1}{t} \cdot \int_0^t C_p^2 dt} \quad (12)$$

2.2 Geometric Variation

The geometric investigation performed here is based on the Constructal Design method seen in Bejan (2000), Dos Santos *et al.* (2017) and Gonzales *et al.* (2021). The method is based on a physical principle, Constructal Law, and used to improve any flow system with finite dimensions. Its principle has application in several knowledge areas as the generation and evolution of geometrical configurations in nature, social organization and engineering. In conjunction with Constructal Design, the exhaustive search method was used as an optimization method, which is a method widely used in recent works, see Letzow *et al.* (2020). It is worth mentioning that Constructal Design is not an optimization method, but a method for geometrical investigation and it has been used for definition of search space of geometric possibilities (Dos Santos *et al.*, 2017; Gonzales *et al.*, 2021). In this sense, several simulations for different geometric variations are performed in the present study.

The geometric evaluation of the present work is performed in the range $0.18 \leq H_2/H_1 \leq 0.81$ with an increment of $\Delta H_2/H_1 = 0.09$. These variations were chosen in order to provide an understanding about the influence of the duct placement over the performance of the idealized OWC device.

2.3 Numerical verification and mesh independence test

Initially, a numerical verification of the spatial and time averaged power coefficient obtained in the study of Akwa (2010) is performed, which analyzed a transient, incompressible, two-dimensional and turbulent airflow of a rectangular free domain with a rotating Savonius turbine inside it. In this check, the results were compared for different Tip Speed Ratios (λ): 0.75; 1.00; 1.25 and 2.00. All thermophysical properties were considered constant and an undisturbed air velocity was adopted at the domain inlet of $V_{cte} = 7$ m/s as well as atmospheric pressure in the geometry air outlet. The Reynolds number for the study was $Re_D = 867,000$. Figure 3 illustrates the effect of the Tip Speed Ratio (λ) over the average power coefficient (C_p) obtained with the present model and that predicted by Akwa (2010).

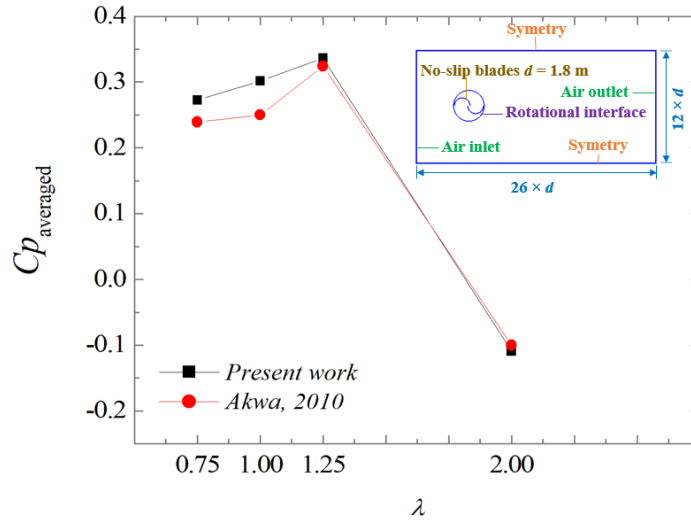


Figure 3. Comparison between the effect of λ over Cp_{averaged} obtained with the present numerical model and that predicted by (Akwa, 2010).

Considering the difficulties in predicting the Cp coefficient due to the complexity of turbulent flows and the vortex shedding generated, which led several uncertainties for prediction of flow parameters as the power coefficient, and the fact that authors used another software, obtained results can be considered satisfactory for the study continuity.

After numerical verification, the OWC device geometry, containing the same rotational moving mesh Savonius turbine configuration, was proposed and a mesh independence test was performed for the first geometric variation analyzed, with $H_2/H_1 = 0.18$. A total of four meshes were tested, evaluating the mean total relative difference pressure into OWC duct over a time interval of 0.5 s, calculated by:

$$\text{Relative difference} = 100 \times \left| \frac{(P_{Total}^{\varepsilon} - P_{Total}^{\varepsilon+1})}{P_{Total}^{\varepsilon}} \right| \quad (13)$$

where P_{Total}^{ε} is the mesh analyzed total pressure [Pa], $P_{Total}^{\varepsilon+1}$ is the subsequently analyzed mesh total pressure and $\varepsilon = 1$ to 4.

The mesh chosen to be evaluated as the independent one was the fourth. The results of the mesh independence test performed are shown in Table 1.

Table 1. Mesh independence test results

Mesh	Mesh size	Pressure [Pa]	Relative difference
1	116,505	436.140	8.908×10^{-2}
2	125,516	435.751	4.855×10^{-2}
3	134,702	435.963	2.593×10^{-2}
4	146,660	435.850	----

The finite volumes independent mesh y^+ values ranged on average to less than 1, including in the surfaces of the turbine. Figure 4 illustrates the chosen mesh for the study, detailing its refinement in the Savonius turbine airfoils region.

All the cases were solved with a pressure-based solver, SIMPLE (Semi-Implicit Linked Equations) algorithm for pressure-velocity coupling, second order spatial discretization for the pressure, second order Upwind for momentum and First Order Upwind for turbulent kinetic energy. The transient formulation used was First Order Implicit. These simulation configurations were adopted due to the better conservation equations and the $k-\omega$ SST turbulence modeling convergence.

The simulations were performed in a computer with an AMD Ryzen 7 3700X 8-Core Processor @ 4.09 GHz and 16 GB of RAM memory. The GMSH software was used to construct all the computational meshes and the Ansys FLUENT 18.1 commercial software was used to solve the conservation equations, where the converged residual solution adopted is 1×10^{-5} , with a time step of $\Delta t = 0.00175$ s and the total simulations flow time of $t = 1.75$ s.

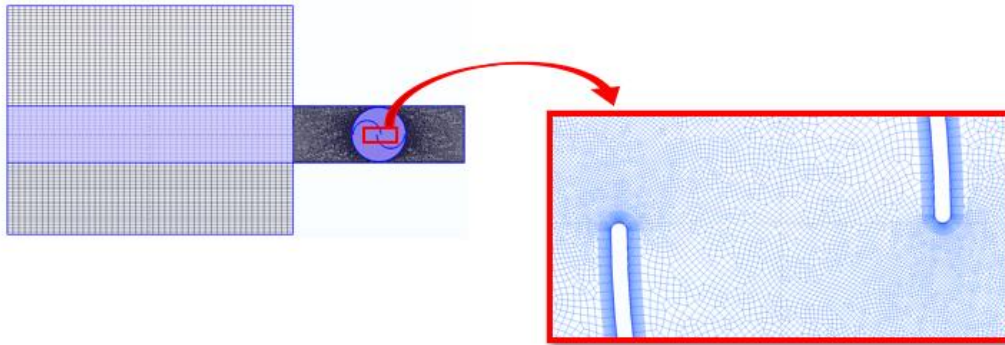


Figure 4. Independent mesh with Savonius turbine airfoils detail.

3. RESULTS AND DISCUSSION

After the mesh independence test, all simulations were performed varying the OWC device duct placement, H_2/H_1 , as mentioned in the previous item of this work. The results for the available RMS hydropneumatic power of the OWC device without and containing a Savonius turbine were calculated in the time interval of $0.68 \text{ s} \leq t \leq 1.75 \text{ s}$ in order to guarantee the stabilization of the flow throughout the domain. The geometry simulations without the Savonius turbine are important to obtain the available power used in the calculation of the power coefficient of the device. Moreover, these simulations allowed performing the comparison between the effect of the ratio H_2/H_1 over the performance of the device with and without the turbine and evaluating whether the use of different geometric domains of the OWC device are important for future design recommendations with the same imposed conditions in this study.

Figure 5 illustrates the velocity field for different positions of turbine duct placed in lateral face chamber of the OWC. All fields are captured for the instant time of $t = 1.75 \text{ s}$.

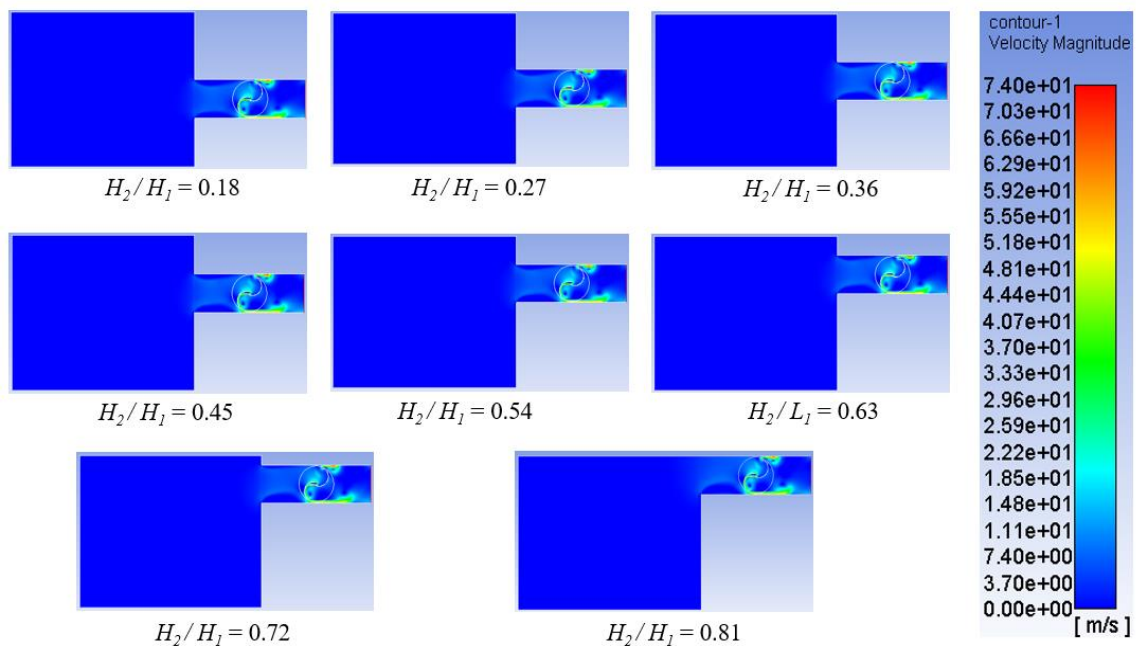


Figure 5. Velocity magnitude fields for the flow with inserted turbine at $t = 1.75 \text{ s}$.

It can be evaluated through the velocity fields in the analyzed model that, in spite of high similarity between the fields, there was a difference in the variation $H_2/H_1 = 0.81$. This difference is caused by the lower air flow recirculation at the top of the hydropneumatic chamber. Moreover, the velocity fields also indicated a detachment of the boundary layer in the two corners for lower magnitudes of H_2/H_1 forcing the fluid flow to pass in the central region of turbine. As the ratio H_2/H_1 increases, the detachment is dominant in the lower corner of the duct, forcing the flow to focus over the advancement blade of Savonius turbine. This behavior is the main responsible here for improvement of device performance.

These differences can be best observed when a comparison between the RMS available hydropneumatic power for different OWC device geometry ratio is performed. In order to show the influence of turbine duct position with a rotational turbine over the device power, Figure 6 shows the effect of the ratio H_2/H_1 over the RMS available power (black line) and RMS turbine power (red line).

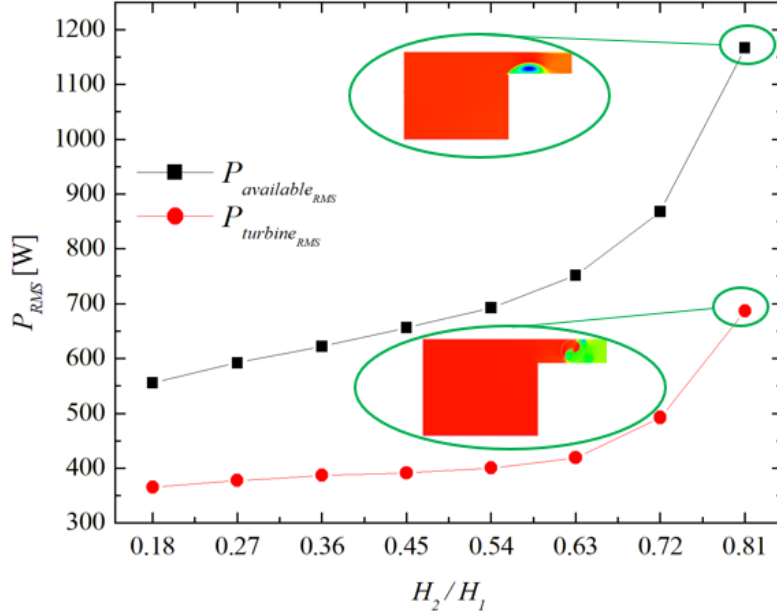


Figure 6. RMS available hydropneumatic power comparison by the RMS Savonius turbine power.

The results obtained for the best geometry were 1,166.76 W for the power available in the equipment without a turbine and 686.85 W for the equipment containing the turbine. These comparative results of Fig. 5 show the importance of design investigation in this kind of problem, since a difference of 46.80% is noticed when the best and worst configurations are compared for the OWC with Savonius turbine geometry variation. Other important aspect is the achievement of similar effects of degrees of freedom over RMS turbine power and RMS available power. Thus, it can be stated that the complexity of adding a moving mesh modeling the Savonius turbine did not significantly affect the influence of OWC device duct position over the device performance, as well as, the optimal configuration, for the present investigated conditions. Therefore, for the present conditions, the simulation of the problem without turbine led to the same optimal geometrical configurations and effect of studied degrees of freedom than that reached for the simulation with turbine. It is worth to mention that the simulation without turbine reduces dramatically the computational effort.

As previously stated, the best result was obtained when $H_2/H_1 = 0.81$, which conducts to a power coefficient of $C_{p_{RMS}} = 0.554$. Concerning the comparison between the cases with different geometries, the best and worst case difference obtained was 8.84%. These results confirm that with lower air flow recirculation due to the positioning of the duct on the equipment hydropneumatic chamber, it induces a higher value for the power coefficient for this geometric configuration of the OWC device. Its also important to note that the $C_{p_{RMS}}$ results in all simulated cases are below the Betz limit of 0.59, according to Kramm *et al.* (2016) and Akwa (2010). The maximum $C_{p_{RMS}}$ obtained here is slight inferior to that predicted by the Betz limit, which indicates that the enclosure can increase the turbine performance in comparison with a free turbine.

4. CONCLUSIONS

In this work, turbulent, incompressible and transient air flow is simulated inside a two-dimensional domain that mimics an OWC device containing a Savonius turbine. The OWC turbine duct is arranged in the horizontal direction, next to the hydropneumatic chamber, in a similar form studied in Letzow *et al.* (2020) and found in other literature works. The geometry is analyzed in order to obtain, as performance indicator, the RMS power coefficient by varying the OWC turbine duct position with a fixed OWC chamber area through the Constructal Design, applying the exhaustive search method for an OWC geometric variation, with one degree of freedom. Constant velocity inlet the device and a rotational moving mesh mimics a Savonius turbine rotor, inside the OWC turbine duct, with constant angular velocity.

Results indicated that, for this study, the once optimized ratio is obtained for $(H_2/H_1)_o = 0.81$ and conducted to once maximized C_p of $(C_{p_{RMS}})_m = 0.554$. For the worst ratio, $H_2/H_1 = 0.18$, it is obtained a $C_{p_{RMS}} = 0.505$. Results showed that the location of the duct in the upper part of the hydropneumatic chamber induced the air flow to focus on the advancement

- Cresesb, “Reference Center for Solar and Wind energy Sérgio de Salvo Brito. Wind energy principles and technologies” (in Portuguese), 2008. Accessed in 25/03/2021: <http://www.cresesb.cepel.br/>.
- Dos Santos, E.D.; Isoldi, L.A.; Gomes, M.N.; Rocha, L.A.O., 2017. “The constructal design applied to renewable energy systems”. In: Rincón-Mejía E, de las Heras A (eds.). Sustainable Energy Technologies. 1 Ed., Boca Raton: CRC Press - Taylor & Francis Group, 63-87.
- Dos Santos, A.L.; Isoldi, L.A.; Rocha, L.A.O.; Gomes, M.N.; Vieira, R.S.; dos Santos, E.D., 2019 “Development of a numerical model for the study of an oscillating water column device considering an impulse turbine”. *Thermal Engineering*, Vol. 18, No. 1, p. 99-105.
- Gomes, M. N., 2014. *Constructal Design for Conversion of Energy from Sea Waves to Electrical Energy of Oscillating Water Column type* (in Portuguese). Doctoral Dissertation, Graduate Program in Mechanical Engineering, Federal University of Rio Grande do Sul, Porto Alegre, Brazil.
- Gonzales, G. V. ; Lorenzini, G. ; Isoldi, L. A. ; Rocha, L. A. O. ; Dos Santos, E. D. ; Silva Neto, A. J. “Constructal Design and Simulated Annealing applied to the geometric optimization of an isothermal Double T-shaped cavity”. *International Journal of Heat and Mass Transfer*, v. 174, p. 121268-19, 2021.
- Jenniches, S., 2018. “Assessing the regional economic impacts of renewable energy sources – A literature review”. *Renewable and Sustainable Energy Reviews*, Vol. 93, pp. 35-51.
- Kramm, G.; Sellhorst, G.; Ross, H. K.; Cooney, J.; Dlugi, R.; Mölders, N., 2016. “On the Maximum of Wind Power Efficiency”. *Journal of Power and Energy Engineering*, Vol. 4, pp. 1-39.
- Letzow, M.; Lorenzini, G.; Barbosa, D.V.E.; Hübner, R.G.; Rocha, L.A.O.; Gomes, M.N.; Isoldi, L.A.; dos Santos, E.D., 2020. “Numerical analysis of the influence of geometry on a large scale onshore oscillating water column device with associated seabed ramp”. *International Journal of Design & Nature and Ecodynamics*, Vol. 15, No. 6, pp. 873-884.
- Maliska, C.R., 2004. *Heat Transfer and Computational Fluid Mechanics* (in Portuguese). 2^a ed. LTC - Livros Técnicos e Científicos, Federal University of Santa Catarina, Florianópolis, Brazil.
- Marjani, A. E.; Castro, F.; Bahaji, M.; Filali, B. "3D Unsteady Flow Simulation in an OWC Wave Converter Plant". ICREPQ' 06. Palma de Mallorca, Spain, 2006.
- Menter, F.R., Kuntz, M., Langtry, R., 2003. “Ten Years of Industrial Experience with the SST Turbulence Model”. *Turbulence, Heat and Mass Transfer* 4 p625-632.
- Patankar, S.V., 1980. “Numerical Heat Transfer and Fluid Flow”. McGraw Hill, New York, USA.
- Pinto Jr, E.A.; Gomes, M.N.; Rocha, L. A. O.; dos Santos, E.D.; Isoldi, L. A., 2019. “Evaluation of Static Pressure Behavior in an Oscillating Water Column Wave Energy Converter”. *RETERM - Engenharia Térmica/ Thermal Engineering* 18, 36–42.
- Savonius, S.J., 1930. UNITED STATES PATENT OFFICE - Sigurd J. Savonius, of Helsingfors, Finland - Wind Rotor.
- Twidell, J., and Weir, T., 2015, “Renewable Energy Resources”. 3th Ed., Taylor & Francis.
- Versteeg, H.K., Malalasekera, W., 2007. “An Introduction to Computational Fluid Dynamics - The Finite Volume Method”. 1st Ed. ed. Longman, England.
- Wilcox, D.C., 2004. “Turbulence Modeling for CFD”. 2nd ed. [Nachdr], La Cañada, Calif: DCW Industries.

7. RESPONSIBILITY NOTICE

The authors are the only responsible for the printed material included in this paper.